Transition Metal Chemistry
https://doi.org/10.1007/s11243-018-0236-2

Crystal structures and spectroscopic properties of copper(II)–dipicolinate complexes with benzimidazole ligands

Petra Masárová[1] · Vladimír Kuchtanin[1] · Milan Mazúr[2] · Ján Moncol[1]

Received: 17 January 2018 / Accepted: 12 April 2018

Abstract
The syntheses, crystal structures and spectroscopic properties of three Cu(II)–dipicolinate complexes with benzimidazole ligands, namely [Cu(bzim)(dipic)(MeOH)] (**1**), $[Cu_2(2\text{-Etbzim})_2(dipic)_2]_n \cdot 0.5nH_2O$ (**2**) and $[Cu_2(2\text{-}^{i}Prbzim)_2(dipic)_2]_n$ (**3**), where dipic = dipicolinate, bzim = 1-H-benzimidazole, 2-Etbzim = 2-ethyl-1-H-benzimidazole and 2-iPrbzim = 2-isopropyl-1-H-benzimidazole, are reported. Crystal structure studies revealed different coordination modes of the dipicolinate ligands; tridentate chelating for monomeric complex **1**, and both tridentate chelating and bridging for similar polymeric complexes **2** and **3**. Polymers **2** and **3** both contain two units, in which the Cu(II) central atoms Cu1 and Cu2 have different coordination polyhedra. The first unit $\{Cu(dipic)_2\}$ with Cu1 is connected to the second via two bidentate carboxylate groups of an μ_3-bridging dipicolinate. In the second unit, Cu2 is coordinated by two imidazole nitrogen atoms from 2-ethyl-1-H-benzimidazole (**2**) or 2-isopropyl-1-H-benzimidazole (**3**) ligands. Complex **2** is of higher symmetry and has a localized Cu(II) atom Cu2 in a special position on the twofold axis. EPR spectra of all three Cu(II) complexes, which were measured at both room temperature and 98 K, indicate distorted tetragonal coordination spheres for all the Cu(II) atoms. The *g*-factor relation ($g_{//} > g_{\perp} > 2.0023$) is consistent with a $d_{x^2-y^2}$ ground electronic state in each case.

Introduction

The design and construction of self-assembled supramolecular architectures and metal–organic frameworks with desired topologies and interesting properties such as catalytic activity, electrical conductivity, magnetic properties, and pharmacological activity [1, 2] constitute a major area of supramolecular chemistry. The many factors which have an influence on the self-assembly of supramolecular structures and metal–organic frameworks include the choice of metal, organic ligands that are capable of intermolecular interactions such as π–π stacking [3] and hydrogen bonding, pH of the solution, choice of solvent, van der Waals forces and others [4, 5]. The selection of organic ligands depends on factors such as steric and electronic effects, flexibility and length of the ligands and position of their functional groups [6].

Benzimidazole and its derivatives are useful *N*-donor ligands for the synthesis of supramolecular architectures, due to their large conjugated π systems and capacity to act as hydrogen bond donors [6]. Furthermore, imidazole and its derivatives are constituents of metalloenzymes [7, 8].

Dipicolinate ligand (dipic = anion derived from pyridine-2,6-dicarboxylic acid) can coordinate with metal ions in a variety of ways. It is a versatile, multidentate ligand with one nitrogen and two oxygen donor atoms and can exhibit a large number of binding modes varying from bidentate or tridentate chelating to bridging via one or more carboxylate oxygen atoms, which leads to many structural variations [9, 10]. Moreover, dipicolinate ligand can behave both as an acceptor and a donor of hydrogen bonds. These properties make dipicolinates valuable ligands in the synthesis of supramolecular coordination compounds [11]. In addition, dipicolinate compounds may exhibit insulin-like properties [12] and superoxide dismutase (SOD) activity [13], they can also activate or inactivate some metalloenzymes, inhibit

Electronic supplementary material The online version of this article (https://doi.org/10.1007/s11243-018-0236-2) contains supplementary material, which is available to authorized users.

✉ Ján Moncol
jan.moncol@stuba.sk

[1] Department of Inorganic Chemistry, Faculty of Chemical and Food Technology, Slovak University of Technology, 812 37 Bratislava, Slovak Republic

[2] Department of Physical Chemistry, Faculty of Chemical and Food Technology, Slovak University of Technology, 812 37 Bratislava, Slovak Republic

Published online: 24 April 2018

electron transport, and function as electron carriers in DNA cleavage [14]. Due to their low toxicity and amphophilic nature, they can serve as models for pharmacologically active compounds [15].

Crystal structures of some dipicolinate complexes with a variety of benzimidazole ligands, similar to the complexes reported in the present work, have been described [16–20].

In this work, we present the synthesis, crystal structures and spectral properties (IR, UV/Vis and EPR) of three new Cu(II)–dipicolinate complexes with various benzimidazole ligands, namely [Cu(bzim)(dipic)(MeOH)] (**1**), $[Cu_2(2\text{-Etbzim})_2(dipic)_2]_n{\cdot}0.5nH_2O$ (**2**) and $[Cu_2(2\text{-}^{i}Prbzim)_2(dipic)_2]_n$ (**3**). The crystal structures of all three complexes are discussed in detail.

Experimental

All the benzimidazole proligands were synthesized as described in our previous paper [21], as follows. A mixture of o-phenylenediamine (0.1 mol) and 0.1 mol of formic acid (for 1-H-benzimidazole), propionic acid (for 2-ethyl-1-H-benzimidazole) or isobutyric acid (for 2-isopropyl-1-H-benzimidazole) was added to 4 M hydrochloric acid (50 cm^3). The resulting mixture was heated for 4 h under reflux. The solution was cooled and the pH was adjusted to 8 with 26% ammonia solution. The solid was collected by filtration, dissolved in 1 M hydrochloric acid, and treated with charcoal. The mixture was filtered and the pH was adjusted to 8 with ammonia solution, and the resulting precipitate was collected by filtration. The filtre cake was washed with cold water to obtain 1-H-benzimidazole in 75% yield, 2-ethyl-1-H-benzimidazole in 85% yield and 2-isopropyl-1-H-benzimidazole in 85% yield, (all white solids).

^{1}H NMR (300 MHz, DMSO-d_6, δ ppm) for 1-H-benzimidazole: 8.21 (s, 1H), 7.64 (dd, $J = 6.0$, 3.2 Hz, 2H), 7.23 (dd, $J = 6.0$, 3.2 Hz, 2H).

^{13}C NMR (75 MHz, DMSO-d_6, δ ppm) for 1-H-benzimidazole: 142.4, 138.9, 122.3, 115.9.

^{1}H NMR (300 MHz, DMSO-d_6, δ ppm) for 2-ethyl-1-H-benzimidazole: 7.50 (dd, $J = 5.9$, 3.2 Hz, 2H), 7.14 (dd, $J = 6.0$, 3.2 Hz, 2H), 2.88 (q, $J = 7.6$ Hz, 2H), 1.38 (t, $J = 7.6$ Hz, 3H).

^{13}C NMR (75 MHz, DMSO-d_6, δ ppm) for 2-ethyl-1-H-benzimidazole: 156.8, 139.6, 121.6, 115.0, 22.6, 12.7.

^{1}H NMR (300 MHz, DMSO-d_6, δ ppm) for 2-isopropyl-1-H-benzimidazole: 7.51 (dd, $J = 6.0$, 3.2 Hz, 2H), 7.15 (dd, $J = 6.0$, 3.2 Hz, 2H), 3.21 (hept, $J = 6.9$ Hz, 1H), 1.41 (d, $J = 6.9$ Hz, 6H).

^{13}C NMR (75 MHz, DMSO-d_6, δ ppm) for 2-isopropyl-1-H-benzimidazole: 160.4, 139.3, 121.7, 115.1, 29.0, 21.9.

The ^{1}H NMR and ^{13}C NMR spectra of the proligands are given in the supplementary materials (see Supplementary Materials Figs. S1–S6).

IR (ATR, cm^{-1}) for 1-H-benzimidazole: 3113(w), 3061(w), 3002(w), 2939(w), 2860(w), 2789(w), 1771(m), 1620(m), 1588(m), 1477(m), 1456(s), 1406(s), 1364(s), 1300(s), 1271(s), 1244(s), 1202(m), 1132(m), 1003(m), 958(m), 887(m), 767(m), 743(s), 634(m), 626(m), 617(m), 578(w), 417(s).

IR (ATR, cm^{-1}) for 2-ethyl-1-H-benzimidazole: 3053(w), 2974(w), 1622(m), 1589(w), 1541(m), 1456(s), 1439(s), 1425(s), 1408(s), 1379(m), 1324(m), 1270(s), 1070(m), 1043(m), 966(m), 881(m), 793(m), 738(vs), 617(m), 476(m), 432(m).

IR (ATR, cm^{-1}) for 2-isopropyl-1-H-benzimidazole: 3049(w), 2968(w), 1622(m), 1591(w), 1537(m), 1456(m), 1411(s), 1389(m), 1360(m), 1321(m), 1273(s), 1228(m), 1213(m), 1093(m), 1016(m), 995(m), 930(w), 868(w), 768(m), 739(vs), 619(m), 449(m), 420(m).

The synthesis of the complexes [Cu(bzim)(dipic)(MeOH)] (**1**), $[Cu_2(2\text{-Etbzim})_2(dipic)_2]_n{\cdot}0.5nH_2O$ (**2**) and $[Cu_2(2\text{-}^{i}Prbzim)_2(dipic)_2]_n$ (**3**) was carried out in the following manner. To a water (40 cm^3, complex **2**) or a methanol (40 cm^3, complexes **1** and **3**) solution of copper(II) acetate monohydrate (0.15 g, 0.75 mmol) was added 1-H-benzimidazole (for **1**, 0.09 g, 0.75 mmol), 2-ethyl-1-H-benzimidazole (for **2**, 0.22 g, 1.5 mmol) or 2-isopropyl-1-H-benzimidazole (for **3**, 0.24 g, 1.5 mmol). The mixture was stirred for 30 min at ambient temperature to obtain a homogeneous solution, then further treated with dipicolinic acid (0.125 g, 0.75 mmol) and heated under reflux. The resulting blue or violet-blue solutions were cooled to ambient temperature, filtered, and left to crystallize. Single crystals of complexes **1**–**3** suitable for X-ray diffraction were formed within a few days.

Complex 1 IR (ATR, cm^{-1}): 3440(w), 3371(w), 3163(w), 3091(w), 2810(w), 2642(w), 1651(s), 1628(s), 1615(s), 1595(s), 1496(m), 1470(w), 1430(m), 1365(s), 1346(s), 1307(m), 1279(m), 1254(m), 1178(m), 1146(w), 1079(m), 1007(w), 984(w), 912(m), 876(m), 848(w), 824(w), 765(s), 750(s), 737(s), 679(s), 635(w), 624(w), 589(w), 548(w), 437(s), 426(s).

Found (calc.): C 47.6 (47.6), N 10.9 (11.1), H 3.7 (3.5).

UV/Vis (nm): 202, 249, 273, 738.

Complex 2 IR (ATR, cm^{-1}): 3182(w), 2978(w), 2654(w), 1630(s), 1614(s), 1579(s), 1489(w), 1454(s), 1427(m), 1371(s), 1280(s), 1182(m), 1080(s), 1051(w), 1005(w), 916(w), 862(w), 819(w), 782(m), 762(w), 734(s), 683(m), 633(w), 436(m).

Found (calc.): C 50.6 (50.1), N 11.4 (11.0), H 3.5 (3.7).

UV/Vis (nm): 215, 246, 279, 547, 755.

Complex 3 IR (ATR, cm^{-1}): 3180(w), 3082(w), 2976(w), 2879(w), 2775(w), 2654(w), 1618(s), 1585(s), 1452(m), 1426(w), 1359(s), 1277(s), 1181(m), 1080(m), 1031(w), 1003(w), 912(w), 862(w), 818(m), 785(m), 762(m), 730(s), 683(m), 434(m).

Found (calc.): C 52.2 (52.5), N 10.0 (10.8), H 4.0 (3.9).

UV/Vis (nm): 205, 248, 279, 560, 749.

The UV/Vis spectra of complexes **1**–**3** are shown in the Supplementary Materials Fig. S7. Complex **1** has a molar absorptivity coefficient at $\lambda = 738$ nm ($\varepsilon_{738} = 86.5$ L mol^{-1} cm^{-1}) (see Supplementary Materials Fig. S8).

Room temperature (RT) values of magnetic moments μ_{eff} for complexes **2** and **3** were obtained as 2.48 μ_B for **2**, indicative of dimeric behaviour in a magnetic field and $\mu_{eff} = 1.76$ μ_B for complex **3**, which corresponds to the spin-only value for $S = ½$ and one unpaired electron in the $3d^9$ system ($\mu_{eff} = 1.73$ μ_B). Decrease of μ_{eff} values below 20 K is caused by zero-field splitting (ZFS), but could also indicate antiferromagnetic exchange interactions between the Cu(II) atoms for **2** and **3** (see Supplementary Materials Figs. S9, S10). The presence of antiferromagnetic exchange coupling between the copper(II) atoms confirms significant deviation from linear behaviour of the function $\chi = f(1/T)$ (see Supplementary Materials Figs. S9, S10).

X-ray crystallography

The data collections for complexes **1**–**3** at 100 K were made with a Stoe StadiVari diffractometer using a Pilatus3R 300 K HPAD detector and microfocus source Xenocs GeniX3D HF with CuKα radiation. The structures were solved using SHELXT [22] or SUPERFLIP [23] and refined by full-matrix least-squares procedures with SHELXL (version 2017/1) [24]. The absorption corrections were made by multi-scan methods using the Stoe LANA programme [25]. Geometrical analyses were performed with SHELXL. The structures were drawn using the OLEX2 package [26]. Crystal data, conditions of data collection and refinement are reported in Table 1. The crystal structure of complex **2** showed disorder of the dipicolinate and 2-ethyl-1-H-benzimidazole ligands. The whole 2-ethyl-1-H-benzimidazole ligand was disordered in two positions [N3–N4/C12–C20] and [N3A–N4A/C12A–C20A] with occupancy factors 0.671(4) (green line) and 0.329(4) (violet line) (see Supplementary Materials Fig. S11). One of two dipicolinate ligands [N1/O1–O4/C1–C7] was disordered around the twofold axis (the two orientations of the dipicolinate ligand are drawn using green and violet lines, see Supplementary Materials Fig. S11). Crystallographic data (excluding structure factors) for the structures reported in this paper have been deposited within the Cambridge Crystallographic Data Centre as supplementary publication nos. 1586345–1586347. Copies

Table 1 Crystallographic data for complexes **1–3**

	1	**2**	**3**
Chemical formula	$C_{15}H_{13}CuN_3O_5$	$C_{32}H_{27}Cu_2N_6O_{8.5}$	$C_{34}H_{30}Cu_2N_6O_8$
M_r	378.82	758.67	777.72
Crystal system	Triclinic	Monoclinic	Monoclinic
Space group	$P\bar{1}$	$C2/c$	Cc
T (K)	100(1)	100(1)	100(1)
a (Å)	6.4426(3)	10.4082(4)	10.3374(3)
b (Å)	10.7774(6)	17.8362(5)	18.0741(4)
c (Å)	11.0318(5)	17.3477(7)	17.9011(5)
(°)	76.570(4)	90	90
β (°)	88.770(4)	94.777(3)	92.401(2)
γ (°)	83.840(4)	90	90
V ($Å^3$)	740.73(6)	3209.3(2)	3341.69(15)
Z	2	4	4
λ (Cu–Kα) (Å)	1.54186	1.54186	1.54186
μ (mm^{-1})	2.394	2.176	2.093
Crystal size (mm)	0.40 × 0.05 × 0.05	0.12 × 0.06 × 0.05	0.16 × 0.09 × 0.05
ρ_{calc} (g cm^{-3})	1.698	1.570	1.546
S	0.995	1.059	1.159
R_1 [$I > 2\sigma(I)$]	0.0567	0.0457	0.0644
wR_2 [all data]	0.1509	0.1279	0.1821
$\Delta\rangle_{max}$, $\Delta\rangle_{min}$/e ($Å^{-3}$)	1.32, −1.29	0.84, −0.95	0.51, −0.88
CCDC	1,586,345	1,586,346	1,586,347

of the data can be obtained free of charge on application to the CCDC, 12 Union Road, Cambridge CB2 1EZ, UK [fax: (internat.) +44 1223336033; e-mail:deposit@ccdc.cam.ac.uk].

Physical measurements

All purchased chemicals and solvents were of analytical grade (Aldrich, Sigma) and used as received. Elemental analyses of carbon, hydrogen and nitrogen were carried out with an automated analyser (Vario, Micro Cube) using a CHNSO FlashEA™ 1112 Automatic Elemental Analyser. The electronic spectra were recorded as Nujol mulls and in methanol solution (10^{-3} M) on a Specord 250 plus, Analytical Jena spectrometer in the range of 200–800 nm at room temperature. IR spectra were measured by ATR technique (4000–400 cm^{-1}) on a Magna FTIR 750, Nicolet spectrophotometer at room temperature. All the magnetic measurements were performed on a SQUID magnetometer (Quantum Design, model MPMS SQUID XL-7). The diamagnetic corrections of the molar magnetic susceptibilities were applied using Pascal's constants. Magnetic data were corrected for background values and then processed into χT product function. EPR spectra of the polycrystalline Cu(II) complexes **1**–**3** were recorded on an X-band (≈9.4 GHz) EMX EPR spectrometer (Bruker, Germany) at both RT and 98 K. A special procedure was used for thin-walled quartz EPR tubes packing and precise positioning within the microwave cavity, as described previously [27, 28]. The spin Hamiltonian parameter values were obtained from the experimental EPR spectra by WinEPR (Bruker, [29]) and then further refined by computer simulation using SimFonia (Bruker, [30]). ^{1}H NMR and ^{13}C NMR spectra were recorded with a Varian INOVA-300 spectrometer (^{1}H, 300 MHz, and ^{13}C, 75 MHz) in DMSO-d_6 at 65 °C.

Results and discussion

Crystal structures

The crystal structure of [Cu(bzim)(dipic)(MeOH)] (**1**) is illustrated in Fig. 1. Selected bond lengths and angles are tabulated in Table 2. The complex crystallizes in the triclinic space group $P-1$. The copper(II) atom in [Cu(bzim)(dipic)(MeOH)] is five-coordinated with a square pyramidal geometry. The molecular structure of [Cu(bzim)(dipic)(MeOH)] consists of a Cu(II) atom in a basal plane formed by the pyridine nitrogen atom and two carboxylate oxygen atoms of a tridentate chelating pyridine-2,6-dicarboxylate anion, and an imidazole nitrogen atom [Cu1–N1 distance of 1.907(3) Å (Table 2), Cu1–O1 distance of 2.018(2) Å (Table 2), Cu1–O3 distance of 2.023(2) Å (Table 2)], and

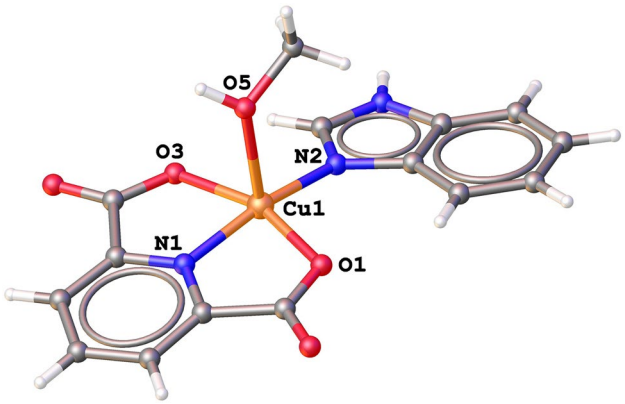

Fig. 1 Molecular structure of complex **1**

Table 2 Selected geometric parameters (Å, °) for **1**

Cu1–O3	2.023(2)	Cu1–O5	2.271(2)
Cu1–O1	2.018(2)	Cu1–N1	1.907(3)
Cu1–N2	1.941(3)		
O3–Cu1–O5	92.17(9)	O1–Cu1–O3	160.54(10)
O1–Cu1–O5	95.02(9)	N2–Cu1–O3	95.38(10)
N2–Cu1–O5	98.91(11)	N2–Cu1–O1	101.31(10)
N1–Cu1–O3	95.60(10)	N1–Cu1–O5	95.45(10)
N1–Cu1–O1	80.74(10)	N1–Cu1–N2	165.23(12)

Cu1–N2 distance of 1.941(3) Å (Table 2)]. The apical position is occupied by the oxygen atom of a methanol ligand [Cu1–O5 distance of 2.271(2) Å (Table 2)]. The crystal structure of a very similar complex [Cu(bzim)(dipic)(H_2O)] with an axial water ligand was published by Dong et al. [20].

The molecules of complex **1** are connected by N–H···O hydrogen bonds between the imidazole NH groups (N3) and uncoordinated carboxylate oxygen atoms (O4) [N3–H3···O4 with an N3···O4 distance of 2.760(3) Å (see Supplementary Materials Table S1)]. There are also O–H···O hydrogen bonds between the methanol oxygen atoms (O5) and uncoordinated carboxylate oxygen atoms (O2) [O5–H5···O2 with an O5···O2 distance of 2.766(4) Å (see Supplementary Materials Table S1)]. In this way, the complex molecules are assembled into 1D supramolecular band chains (Fig. 2).

The principal structural features of $[Cu_2(2\text{-}Etbzim)_2(dipic)_2]_n \cdot 0.5nH_2O$ (**2**) and $[Cu_2(2\text{-}^{i}Prbzim)_2(dipic)_2]_n$ (**3**) are illustrated in Figs. 3 and 4, respectively. Complexes **2** and **3** crystallize in the monoclinic space groups *C*2/c and *Cc*, respectively. Both compounds form similar 1D coordination chains, with two different coordination polyhedra around the copper(II) atoms (Figs. 3, 4). The crystal structure of centrosymmetric complex **2** contains 1D coordination chains and also uncoordinated water molecules (Fig. 3). The 1D coordination chains

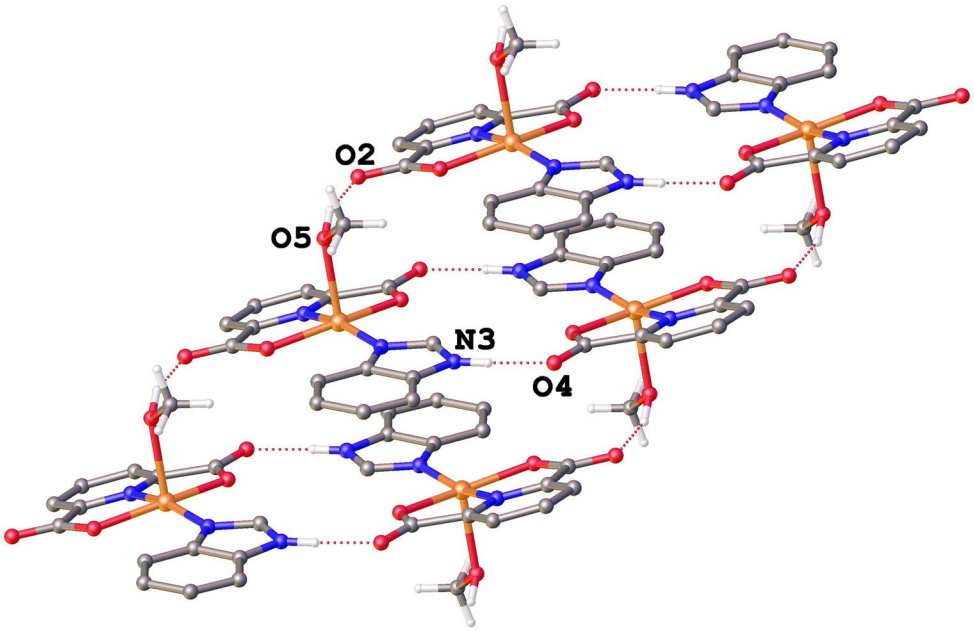

Fig. 2 1D Supramolecular chain structure of complex **1**. The hydrogen atoms are omitted for clarity

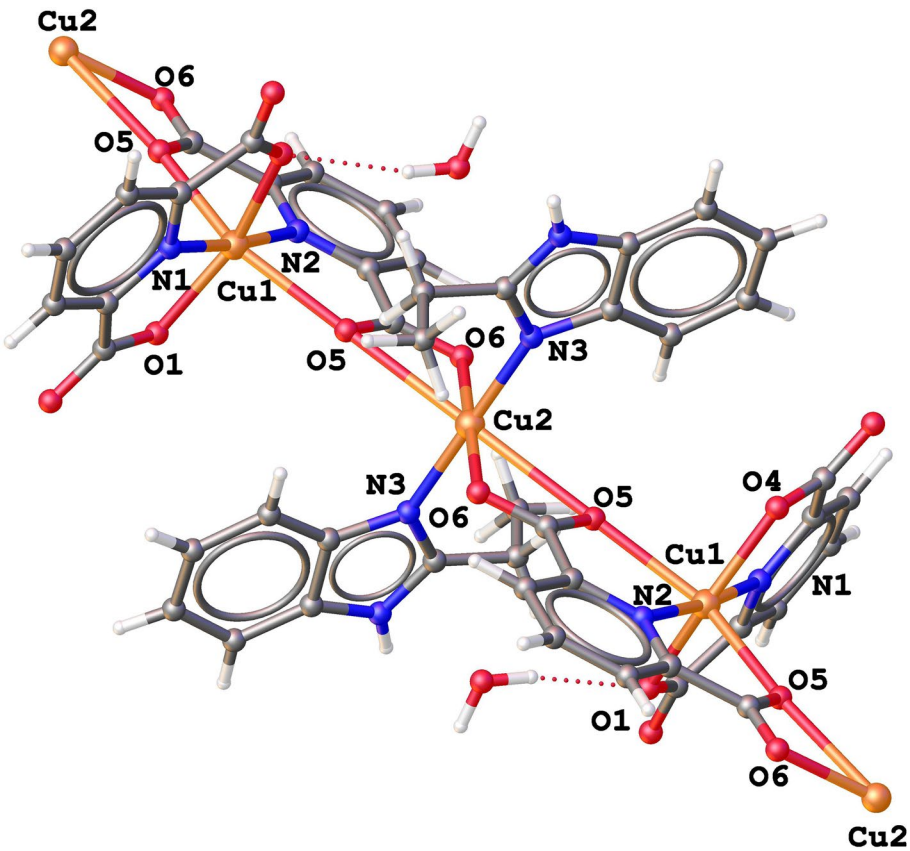

Fig. 3 Molecular structure of complex **2**

are in both cases formed by copper(II) atoms (Cu2) coordinated by two imidazole nitrogen atoms from 2-ethyl-1-H-benzimidazole (**2**) or 2-isopropyl-1-H-benzimidazole (**3**) ligands, and bridged by $\{Cu(dipic)_2\}$ units containing Cu1 atoms, which are bonded to the Cu2 atoms by two bidentate carboxylate groups (Figs. 3, 4). The copper(II) atoms (Cu1) are in both cases six-coordinated by two tridentate dipicolinate ligands, through two pyridine nitrogen atoms (N1, N2) [Cu1–N bond distances are in the range of 1.874(2)–1.995(7) Å (Tables 3, 4)] and four carboxylate

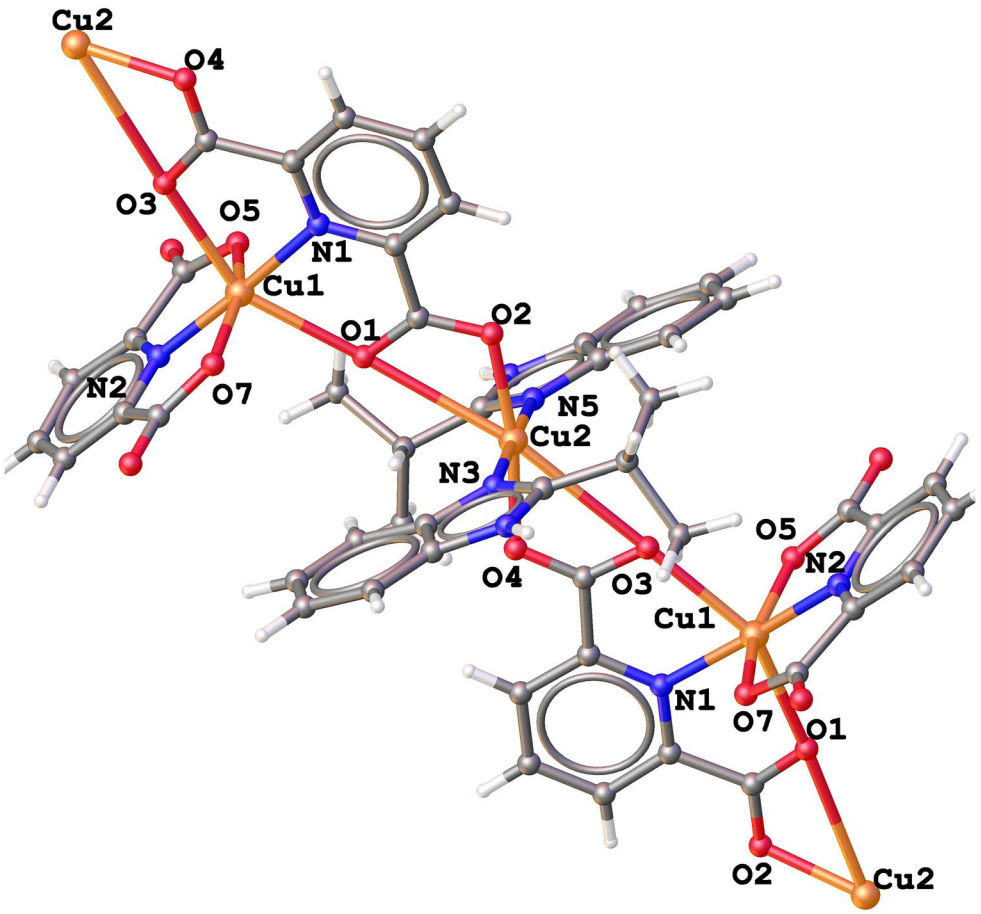

Fig. 4 Molecular structure of complex **3**

oxygen atoms [O1, O4 and 2 × O5 for **2** (Fig. 3), and O1, O3, O5 and O7 for **3** (Fig. 4). The Cu1–O bond lengths are in the range of 2.025(6)–2.381(6) Å (Tables 3, 4)]. One of the dipicolinate ligands in both complexes acts as a tridentate chelating terminal ligand, and the second is μ_3-bridging (tridentate to Cu1, and bidentate to two Cu2 atoms). The Cu2 atoms in both cases are coordinated by two pairs of carboxylate oxygen atoms and two imidazole nitrogen atoms of 2-ethyl-1-H-benzimidazole ligands (complex **2**, Fig. 3) or 2-isopropyl-1-H-benzimidazole ligands (complex **3**, Fig. 4) in an elongated tetragonal bipyramid.

In complex **2**, atom Cu2 is localized in a special position on the twofold axis. The Cu2 atoms of both complexes **2** and **3** are bonded in a *trans* square planar arrangement to the imidazole nitrogen atoms of two disordered 2-ethyl-1-H-benzimidazole ligands (2 × N3 for main part, Fig. 3, or 2 × N3A for minor part) or two 2-isopropyl-1-H-benzimidazole ligands (N3 and N5, Fig. 4) [Cu2–N distances are in the range 1.964(4)–1.977(8) (Tables 3, 4)], plus one carboxylate oxygen atom from two bridging dipicolinate ligands of {Cu(dipic)$_2$} units (2 × O6 for **2** (Fig. 3) or O2 and O4 for **3** (Fig. 4)) [Cu2–O distances are in the range 1.964(6)–1.977(3) (Tables 3, 4)]. The remaining two carboxylate oxygen atoms are strongly [2 x O5 for **2** (Cu2–O5 distance of 2.634(2) Å)] or weakly bonded [O1 and O3 for **3** (Cu2–O distances of 2.892(6) and 2.935(6) Å, respectively] to Cu2. The one disordered dipicolinate ligand around the special position of complex **2** is occasioned by the localization of atom Cu2 on the twofold axis of the crystal structure.

The coordination polymers **2** and **3** are connected through N–H···O hydrogen bonds between the imidazole nitrogen and carboxylate oxygen atoms [N···O distances are in the range of 2.728(15)–2.911(15) Å (see Supplementary Materials Table S1)] into 2D supramolecular frameworks (Figs. 5, 6). The crystal structure of complex **2** also includes O–H···O hydrogen bonds between solvent water molecules (O1W) and carboxylate oxygen (O1 or O4) or neighbouring solvent water molecules (O1W) [O···O distances are in the range 2.78(4)–3.06(3) Å (see Supplementary Materials Table S1)].

IR, UV/Vis and EPR spectroscopy

The IR spectra of complexes **1**–**3** exhibit some similar features. Vibrational bands observed at 3163, 3182 and 3180 cm^{-1} for **1**, **2** and **3**, respectively, are attributed to the N–H stretching vibrations of the benzimidazole ligands. The spectrum of complex **1** also shows stretching vibrations assigned to the O–H groups at 3440 and at 3371 cm^{-1}

Table 3 Selected geometric parameters (Å, °) for **2**

Cu1–O5	2.346(2)	Cu1–O5^{i}	2.346(2)
Cu1–O1	2.046(4)	Cu1–O4	2.046(4)
Cu1–N1	1.874(2)	Cu1–N2	1.988(3)
Cu2–O5	2.634(2)	Cu2–O5^{ii}	2.634(2)
Cu2–O6	1.977(3)	Cu2–O6^{ii}	1.977(3)
Cu2–N3	1.972(3)	Cu2–N3^{ii}	1.972(3)
Cu2–N3A	1.964(4)	Cu2–N3A^{ii}	1.964(4)
O5–Cu1–O5^{i}	150.97(11)	N2–Cu1–O5	75.49(5)
N2–Cu1–O5^{i}	75.49(5)	N2–Cu1–O1	98.9(11)
N2–Cu1–O4	100.9(10)	O1–Cu1–O5	95.8(13)
O1–Cu1–O5^{i}	88.6(12)	O1–Cu1–O4	159.4(7)
N1–Cu1–O5	110.09(19)	N1–Cu1–O5^{i}	98.91(19)
N1–Cu1–N2	174.01(15)	N1–Cu1–O1	82.9(11)
N1–Cu1–O4	76.8(10)	O4–Cu1–O5	94.5(12)
O4–Cu1–O5^{i}	91.0(13)	O5–Cu2–O5^{ii}	180.0
O5^{ii}–Cu2–O6	124.31(8)	O5–Cu2–O6^{ii}	124.31(8)
O5–Cu2–O6	55.69(8)	O5^{ii}–Cu2–O6^{ii}	55.69(8)
O6–Cu2–O6^{ii}	180.0	N3^{ii}–Cu2–O5^{ii}	93.4(4)
N3–Cu2–O5	93.4(4)	N3–Cu2–O5^{ii}	86.6(4)
N3^{ii}–Cu2–O5	86.6(4)	N3^{ii}–Cu2–O6^{ii}	88.6(3)
N3–Cu2–O6	88.6(3)	N3^{ii}–Cu2–O6	91.4(3)
N3–Cu2–O6^{ii}	91.4(3)	N3–Cu2–N3^{ii}	180.0
N3A–Cu2–O5	91.7(7)	N3A^{ii}–Cu2–O5	88.3(7)
N3A–Cu2–O6	92.4(7)	N3A^{ii}–Cu2–O6	87.6(7)
N3A–Cu2–N3A^{ii}	180.0		

Symmetry codes: (i) $-x+1$, y, $-z+3/2$; (ii) $-x+1/2$, $-y+1/2$, $-z+1$

Table 4 Selected geometric parameters (Å, °) for **3**

Cu1–O5	2.027(6)	Cu1–O3	2.368(6)
Cu1–O1	2.381(6)	Cu1–O7	2.025(6)
Cu1–N1	1.995(7)	Cu1–N2	1.923(7)
Cu2–O1	2.892(6)	Cu2–O2	1.965(6)
Cu2–O3^{iii}	2.935(6)	Cu2–O4^{iii}	1.964(6)
Cu2–N3	1.977(8)	Cu2–N5	1.969(7)
O1–Cu1–O3	150.4(2)	O1–Cu1–O5	94.4(2)
O3–Cu1–O5	88.5(2)	O1–Cu1–O7	91.7(2)
O3–Cu1–O7	95.3(2)	O5–Cu1–O7	160.4(2)
N1–Cu1–O1	74.9(2)	N1–Cu1–O3	75.6(3)
N1–Cu1–O5	102.1(3)	N1–Cu1–O7	97.5(3)
N2–Cu1–O1	108.3(3)	N2–Cu1–O3	101.3(3)
N2–Cu1–O5	80.3(3)	N2–Cu1–O7	80.2(3)
N1–Cu1–N2	176.0(3)	O1–Cu2–O3^{iii}	169.2(2)
O1–Cu2–O2	50.9(2)	O2–Cu2–O3^{iii}	139.7(2)
O1–Cu2–O4^{iii}	119.6(2)	O2–Cu2–O4^{iii}	170.5(3)
O3^{iii}–Cu2–O4^{iii}	49.8(2)	N3–Cu2–O2	90.2(3)
N5–Cu2–O2	91.9(3)	N3–Cu2–O4^{iii}	89.2(3)
N5–Cu2–O4^{iii}	88.7(3)	N3–Cu2–O1	89.8(3)
N3–Cu2–O3^{iii}	91.7(3)	N5–Cu2–O1	91.6(2)
N5–Cu2–O3^{iii}	86.6(2)	N3–Cu2–N5	177.9(3)

Symmetry code: (iii) $x+1/2$, $-y+3/2$, $z+1/2$

from the methanol ligand. The aromatic and aliphatic υ(C–H) stretching vibrations are observed at 3091–3082 and at 2978–2810 cm^{-1}, respectively [31].

Very intense vibrational bands around 1630–1579 and 1371–1346 cm^{-1}, respectively, for complexes **1**–**3** should correspond to the asymmetric ν_{as}(COO) and symmetric ν_{s}(COO) stretching vibrations of the carboxylate groups, but their correct identification is ambiguous due to overlapping and interfering bands, as well as involvement of the carboxylate groups in the O–H···O hydrogen bonding networks. Moreover, in the case of polymeric compounds **2** and **3** several different vibrational bands for the carboxylate groups are expected, as a consequence of their diverse coordination modes. The values of $\Delta\nu = \nu_{as}(\mathrm{COO}) - \nu_{s}(\mathrm{COO})$ vary in the range of 208–282 cm^{-1} indicating according to Deacon et al. [32] unidentate binding of the carboxylate groups. This is consistent with the single crystal X-ray structure of **1**, but complexes **2** and **3** also revealed chelating and bridging coordination modes of some carboxylate groups. Therefore, for complexes **2** and **3** peaks at 1454 and 1452 cm^{-1}, respectively, have been tentatively ascribed to the symmetric ν_{s}(COO) stretching vibrations of the carboxylate groups. In this case, the corresponding $\Delta\nu$ values for complexes **2** and **3** are also in the range of 125–176 cm^{-1}.

The solid-state electronic spectra show four (complex **1**) or five (complexes **2** and **3**) maxima. All three complexes exhibit absorption bands in the ranges of 202–215, 246–249 and 273–279 nm in the ultraviolet region, which can be assigned to the $\pi \rightarrow \pi^*$ and $n \rightarrow \pi^*$ intraligand charge transfer transitions of dipicolinate and benzimidazole. In the visible region, one absorption band was observed for the monomeric compound **1**, whereas polymeric compounds **2** and **3** with elongated tetragonal bipyramidal geometries around Cu2 both gave two absorption bands. Broad bands centred at 738–755 and 547–560 nm (for **2** and **3**) correspond to the d–d transitions of the Cu(II) atoms, with $\{CuN_2O_2O'\}$ or $\{CuN_2O_4\}$ chromophores, respectively. The observation of two absorption bands for the d–d transitions of Cu(II) for complexes **2** and **3** is the result of Jahn–Teller distortion, which causes splitting of the bands in the UV/Vis spectrum due to reduction in symmetry (O_h to D_{4h}) [33].

The experimental and computer simulated EPR spectra of complexes **1**–**3**, which were recorded at (**a**) room temperature and (**b**) 98 K, are shown in Fig. 7. Unresolved hyperfine splitting is observed in all the EPR spectra. In Table 5, the *g*-factor values, which were evaluated from the experimental EPR spectra and then further refined by computer simulation, are summarized. At both temperatures, the line shapes of the EPR spectra for each

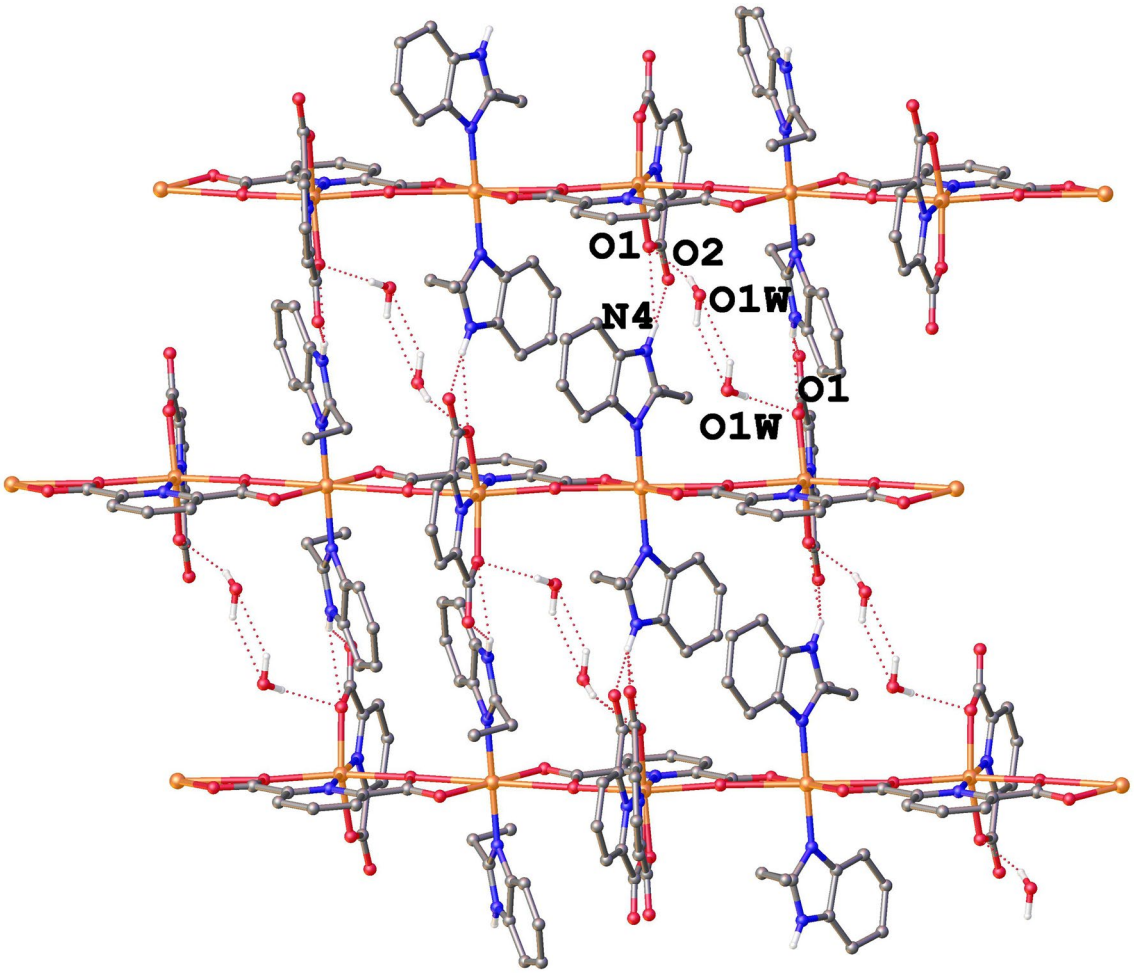

Fig. 5 2D supramolecular framework structure of complex **2**. The hydrogen atoms are omitted for clarity

complex are very similar, and likewise the corresponding *g*-factor values are (within experimental errors) identical. The EPR spectra of complexes **1** and **2** exhibit axial symmetry features. However, orthorhombic EPR spectra were obtained in the case of complex **3**. The axially symmetric EPR spectra of complexes **1** and **2** show the usual relation ($g_{//} > g_{\perp} > 2.0023$), which is consistent with a $d_{x^2-y^2}$ ground electronic state.

The average *g*-factor, g_{av} [34] and geometric parameter, *G* [35] were calculated for each axially symmetric EPR spectrum, as given in Table 5. In the case of complex **1**, the relation $G > 4$ indicates negligible exchange interaction between the Cu(II) centres. However, for complex **2**, the relation $G < 4$ indicates the presence of some exchange coupling between the Cu(II) atoms [35, 36]. The obtained *g*-values are in a good accordance with those reported for similar Cu(II) complexes in the literature [35–37].

Conclusion

Cu(II)–dipicolinate complexes with different benzimidazoles as *N*-donor ligands, namely [Cu(bzim)(dipic)(MeOH)] (**1**), $[Cu_2(2\text{-Etbzim})_2(dipic)_2]_n \cdot 0.5nH_2O$ (**2**) and $[Cu_2(2\text{-}^{i}Prbzim)_2(dipic)_2]_n$ (**3**), were synthesized and structurally characterized by single crystal X-ray diffraction analysis. Complex **1** is a monomer of square pyramidal geometry (4 + 1) with a methanol ligand in the apical position, while complexes **2** and **3** are polymers with similar crystal structures. The dipicolinate in **2** and **3** acts as both tridentate chelating terminal, and a μ_3-bridging ligand. Both polymeric complexes consist of two units with different coordination polyhedra around Cu(II). The copper(II) atoms, Cu1 from the first unit $\{Cu(dipic)_2\}$ and Cu2 from the second unit, made up of Cu2 atom coordinated by two

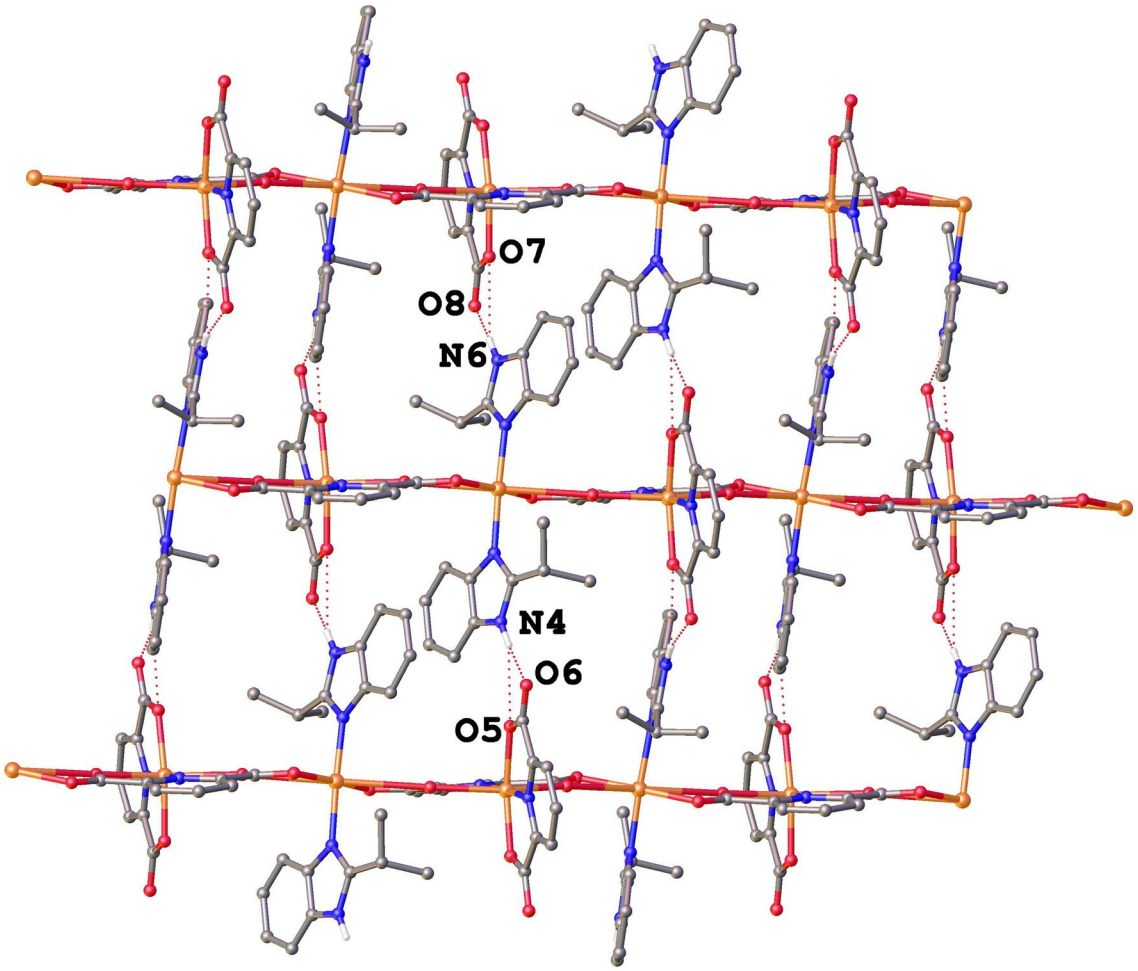

Fig. 6 2D supramolecular framework structure of complex **3**. The hydrogen atoms are omitted for clarity

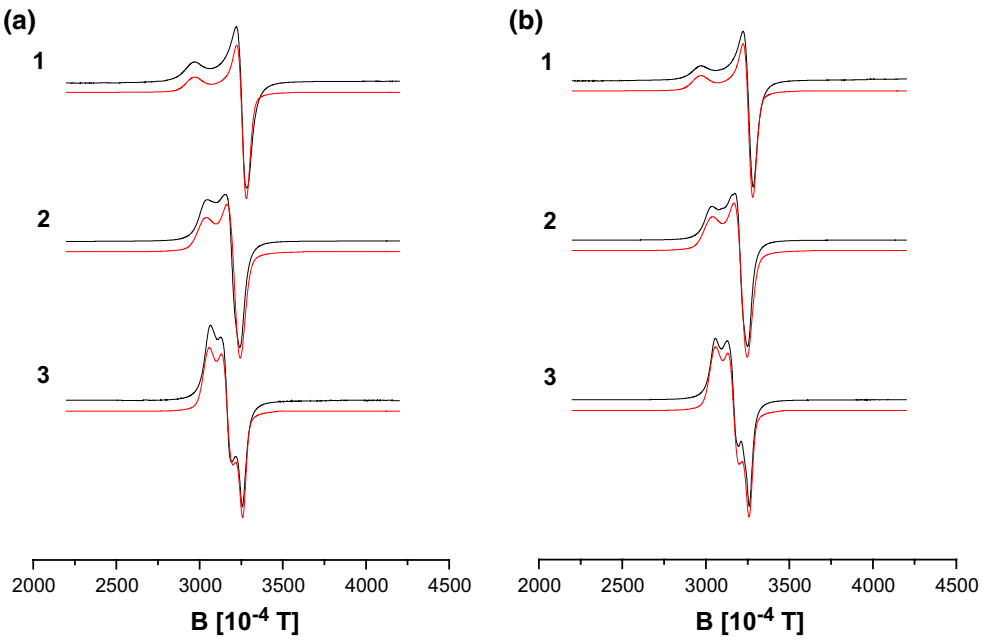

Fig. 7 The experimental EPR spectra of polycrystalline copper(II) complexes **1**–**3** measured at **a** room temperature, **b** 98 K (black line), together with calculated EPR spectra (red line). The spectral parameters for the best fit are given in Table 5. (Color figure online)

Table 5 The EPR parameters of copper(II) complexes **1**–**3**

Copper(II) complex	EPR parameters				
	$g\perp$ (±0.002)		$g\vert$ (±0.002)	g_{av}	G
1	2.063		2.274	2.134	4.33
2	2.088		2.224	2.133	2.55
	$\boldsymbol{g_1}$ (±0.002)	$\boldsymbol{g_2}$ (±0.002)	$\boldsymbol{g_3}$ (±0.002)	$\boldsymbol{g_{av}}$	–
3	2.061	2.132	2.208	2.134	–

The g-factor values obtained for each complex measured at RT and at 98 K are (within experimental error) identical

$g_{av}=(2\,g\perp+g\vert)/3$, $g_{av}=(g_1+g_2+g_3)/3$, $G=(g\vert-2)/(g\perp-2)$

imidazole nitrogen atoms from 2-ethyl-1-H-benzimidazole (**2**) or 2-isopropyl-1-H-benzimidazole (**3**) ligands, are connected to each other via two pairs of carboxylate oxygen atoms from μ_3-bridging dipicolinate. The EPR spectra of the complexes indicate distorted tetragonal coordination spheres for the Cu(II) atoms, with a $d_{x^2-y^2}$ ground electronic state. This work contributes to our knowledge of Cu(II)–dipicolinates containing benzimidazoles, their crystal structures and spectroscopic properties.

Acknowledgements The authors would like to thank Dr. Michal Šoral for recording ^{1}H NMR and ^{13}C NMR spectra of organic proligands and Dr. Ivan Šalitroš for carrying out magnetic measurements. This work was supported by the Slovak Research and Development Agency under the Contact Nos. APVV-15-0053, APVV-16-0039 and APVV-14-0078, the Scientific Grant Agency of the Slovak Republic (Projects VEGA 1/0686/17, VEGA 1/0026/18 and 1/0639/18) and by the STU Grant scheme for Support of Young Researchers (1687). This article was created with the support of the MŠVVaŠ of the Slovak Republic within the Research and Development Operation Programme for the project "University Science Park of STU Bratislava" (ITMS Project No. 26240220084) cofounded by the European Regional Development Fund.

References

1. Cui G-H, Liu T-F, Peng X (2011) J Chem Crystallogr 41:322–327
2. Ghosh SK, Ribas J, Bharadwaj PK (2004) CrystEngComm 6:250–256
3. Janiak C (2000) J Chem Soc, Dalton Trans 21:3885–3896
4. Manna SC, Zangrando E, Chaudhuri NR (2008) J Mol Struct 877:145–151
5. Abdolmaleki S, Ghadermazi M, Fattahi A, Sheshmani S (2016) Inorg Chim Acta 443:284–298
6. Yang R, Li HH, van Hecke K, Cui G-H (2015) Z Anorg Allg Chem 641:642–649
7. Ang HG, Kwik WL, Hanson GR, Crowther JA, McPartlin M, Choi N (1991) J Chem Soc, Dalton Trans 1:3193–3201
8. Subramanian PS, Suresh E, Shukla RS (2005) Inorg Chim Acta 358:2651–2660
9. Mistri S, Zangrando E, Manna SC (2013) Inorg Chim Acta 405:331–338
10. Das B, Baruah J-B (2012) Polyhedron 31:361–367
11. van Albada GA, Ghazzali M, Al-Farhan K, Bouwman E, Reedijk J (2013) Polyhedron 52:1059–1064
12. Yang L, Crans DC, Miller SM, la Cour A, Anderson OP, Kaszynski PM, Godzala ME, Austin LTD, Willsky GR (2002) Inorg Chem 41:4859–4871
13. Siddiqi ZA, Khalid M, Kumar S, Shahid M, Noor S (2010) Eur J Med Chem 45:264–269
14. Tabatabaee M, Bordbar M, Ghassemzadeh M, Tahriri M, Tahrir M, Lighvan ZM, Neumüller B (2013) Eur J Med Chem 70:364–371
15. Gonzalez-Baró AC, Castellano EE, Piro OE, Parajón-Costa BS (2005) Polyhedron 24:49–55
16. Kong F, Yu Z (2011) Acta Crystallogr E67:m783
17. Liu SH, Li YZ, Meng QJ (2005) Acta Crystallogr E61:m1183–m1184
18. Li YH, Li FF, Liu XH, Zhao LY (2012) Acta Crystallogr E68:m739
19. Feng R, Yang Y, Lu Z, Lu F-Y, Nie F-M (2015) Z Kristallogr 230:201–202
20. Dong GY, Fan LH, Yang LX, Khan IU (2010) Acta Crystallogr E66:m532
21. Puchoňová M, Kuchtanin V, Mazur M, Valigura D (2016) Acta Chim Slovaca 9:23–27
22. Sheldrick GM (2015) Acta Crystallogr A 71:3–8
23. Palatinus L, Chapuis G (2007) J Appl Crystallogr 40:786–790
24. Sheldrick GM (2015) Acta Crystallogr C 71:3–8
25. Koziskova J, Hahn F, Richter J, Kozisek J (2016) Acta Chim Slovaca 9:136–140
26. Dolomanov OV, Bourhis LJ, Gildea RJ, Howard JAK, Puschmann H (2009) J Appl Crystallogr 42:339–341
27. Mazur M, Valko M, Morris H, Klement R (1996) Anal Chim Acta 333:253–265
28. Mazur M, Morris H, Valko M (1997) J Magnet Reson 129:188–200
29. Thiele H, Etstling J, Such P, Hoefer P (1992) WINEPR Germany, Bruker Analytic GmbH
30. Weber RT (1995) WINEPR SimFonia. EPR Division, Bruker Instr Inc., Billerica
31. Nakamoto K (1978) Infrared and Raman spectra of inorganic and coordination compounds. Wiley, New York
32. Deacon GB, Phillips RJ (1980) Coord Chem Rev 33:227–250
33. Uma V, Kanthimathi M, Weyhermuller T, Nair BU (2005) J Inorg Biochem 99:2299–2307
34. Weil JA, Bolton JR, Wertz JE (1994) Electron paramagnetic resonance: elementary theory and applications. Wiley, New York
35. Hathaway BJ, Tomlinson AAG (1970) Coord Chem Rev 5:1–43
36. Hathaway BJ, Billing DE (1970) Coord Chem Rev 5:143–207
37. Goodman BA, Raynor JB (1970) Adv Inorg Chem Radiochem 13:135–362